ELSEVIER

PII: S0266-8920(98)00005-8

Prob. Engng. Mech. Vol. 13, No. 4, pp. 309–319, 1998

0266-8920/98 $19.00+0.00

Probabilistic treatment of fracture using two failure models

Claudio Ruggieri

Department of Naval Architecture and Ocean Engineering, University of São Paulo, São Paulo SP 05508-900, Brazil

A probabilistic methodology for brittle fracture based on two local failure models is presented. Probabilistic fracture parameters are obtained using a weakest link and a chain-of-bundles formulation. Both models define limiting distributions for the fracture stress described by a two-parameter Weibull distribution. Numerical procedures employing measured toughness data and finite element solutions are also described to calibrate the Weibull parameters. An application of the methodology then follows to predict geometry and stable crack growth effects on the distribution of macroscopic fracture toughness (J_c) for a high-strength steel. Measured fracture toughness values for a high-constraint geometry that exhibit no prior ductile tearing are effectively 'transferred' to a different geometry having much lower constraint and in which tearing precedes cleavage. The inherent difficulty in predicting the scatter of experimental fracture toughness, as well as constraint and ductile tearing effects, within the scope of conventional procedures appears greatly reduced in the framework presented in this work.

1 INTRODUCTION

The fracture behavior of structural components subjected to various loading and environmental conditions is of obvious relevance in assessing structural integrity. The increasing demand for ensuring acceptable levels of structural safety has spurred a flurry of predictive methodologies aimed at quantifying the impact of defects in load-bearing materials such as, for example, cracks in critical weldments of high-pressure vessels. Such methodologies play a key role in repair decisions and life-extension programs for in-service structures (e.g. aerospace, nuclear and offshore structures). While mechanical failures in structural members and components may result from a combination of several material degradation processes, assessments of structural integrity generally focus on cleavage fracture. This failure mode potentially limit the load bearing capacity of the structure as local crack-tip instability may trigger catastrophic failure at low applied stresses with little plastic deformation.

It has become apparent over recent years that conventional methods of fracture mechanics analysis have limited ability to assess structural integrity in a realistic manner. Most often, these methods are conservative (i.e. the failure of a cracked component at a given load is overpredicted) since they assume conditions rarely experienced by the structure. Further, cleavage fracture is a highly localized phenomenon which exhibits strong sensitivity to material characteristics at the microlevel. In particular, the random inhomogeneity in local features of the material causes large scatter in experimentally measured values of fracture toughness (K_{Ic}, J_c, δ_c or CTOD). Such features make assessments of structural integrity using laboratory testing of standard specimens and simplified crack configurations a complex task: what is the 'actual' material toughness and how is the scatter in measured values of fracture toughness incorporated in procedures for defect assessments?

There has recently been a surge of interest in analysing and predicting material failure caused by transgranular cleavage based upon a probabilistic interpretation of the fracture process. A primary impetus for bringing probabilistic fracture mechanics concepts into play is the inherent random nature of fracture. Attention has been primarily focused on probabilistic models incorporating weakest link statistics. Batdorf and Crose,[1] Evans[2] and Matsuo[3] first considered models of this type to describe brittle fracture for arbitrary loading. Here, a function representing the number of microcracks per unit volume failing at each value of the local tensile stress is used to arrive at the probability of fracture for a cracked body. Later, Beremin,[4] Wallin *et al.*,[5–8] Lin *et al.*,[9] Brückner *et al.*,[10] Godse and Gurland[11] among others provided a link between the size of carbides particles dispersed in the material and the inhomogeneous stress fields ahead of a macroscopic crack. They sought to predict the dependence of fracture toughness (K_{Ic}) on material

properties and temperature. In particular, the work of Beremim[4] and Mudry[12] introduces the Weibull stress (σ_w) as a suitable crack-tip parameter incorporating a local criterion for fracture. More recent efforts in this area have focused on developing transferability models for cleavage fracture toughness based upon the Beremin's Weibull stress. Bakker and Koers,[13] Minami *et al.*,[14] Ruggieri *et al.*,[15,16] assess effects of specimen thickness and crack length on elastic–plastic fracture toughness (J_c, δ_c). Further studies by Ruggieri and Dodds[17–19] generalize the Weibull stress for stationary and growing cracks to include effects of loss of constraint and ductile tearing on macroscopic fracture toughness.

The objectives in developing probabilistic models to describe unstable crack propagation are essentially two fold. First, for a structure containing cracks of different sizes and subjected to complex loading histories, we seek to determine limiting distributions for the (local) fracture stress which couple remote loading (as measured by J or CTOD) with the operative fracture mechanism at the micro-level. In the context of probabilistic models, a fracture parameter associated with the limiting distribution then describes macroscopic fracture behavior for a wide range of loading conditions and crack configurations. As a second objective, we seek to predict unstable crack propagation in larger flawed structures on the basis of a probabilistic fracture parameter. Experimentally measured values of fracture toughness for one configuration (e.g. small laboratory specimens) are rationally extended to predict unstable crack propagation for other crack configurations, provided similarities in both limiting distributions for such a fracture parameter exist.

The plan of the paper is as follows. We first present a probabilistic model to describe fracture in brittle materials and introduce two probability distributions for the fracture stress of cracked bodies. The first distribution derives from the well-known weakest link model while the second one builds upon a chain-of-bundles model. Next, we briefly describe the procedure to calibrate the Weibull parameters of the resulting asymptotic distributions for both failure models. The paper then provides an illustrative application of the methodology to predict geometry and stable crack growth effects on the distribution of macroscopic fracture toughness (J_c) for a high-strength steel. A short discussion on the results and its implications for brittle fracture assessments of load-bearing materials concludes this study.

2 PROBABILISTIC MODEL FOR CLEAVAGE FRACTURE

2.1 Failure probability for a cracked solid

We consider an arbitrarily stressed body where a macroscopic crack lies in a material containing randomly distributed flaws as illustrated in Fig. 1. The fracture process zone ahead of the crack tip is defined as the highly stressed region where the local operative mechanism for cleavage takes place; this region contains the potential sites for cleavage cracking. For the purpose of developing a probabilistic model for brittle fracture, we divide the fracture process zone ahead of crack tip in N unit volumes statistically independent, V_i, $i = 1,2,\ldots,N$. Each unit volume contains a substantial number of statistically independent microflaws uniformly distributed.

The statistical nature of brittle fracture underlies a simplified treatment for unstable crack propagation of the configuration represented in Fig. 1(a). We first limit attention to the asymptotic distribution for failure of the unit volume and consider V divided into small volumes uniformly stressed statistically independent δV_j, $j = 1,2,\ldots,n$, as illustrated in Fig. 1(b). Let p denote the probability of failure for the jth volume δV_j. The probability that k failures occur (which

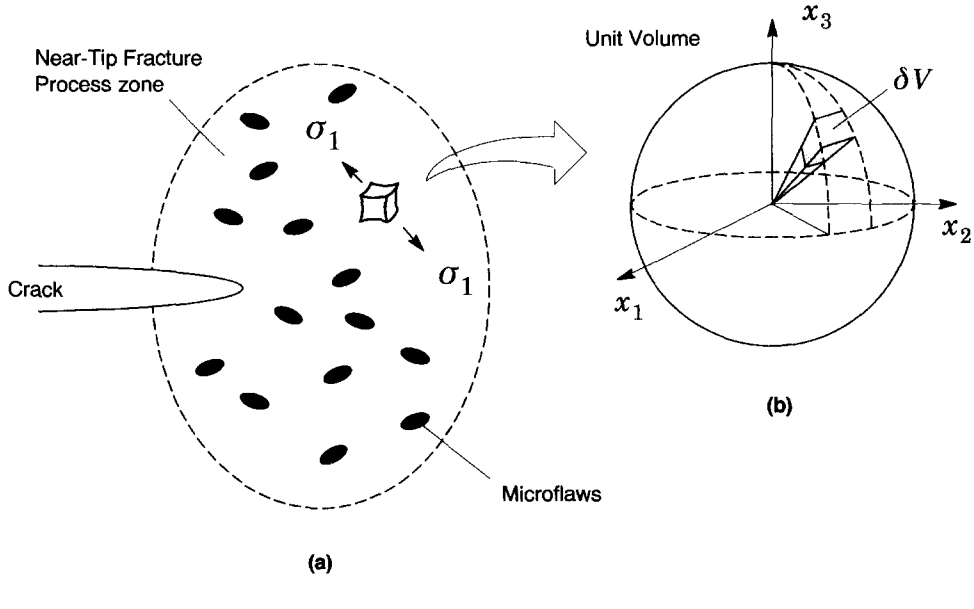

Fig. 1. (a) Fracture process zone ahead of a macroscopic crack containing randomly distributed flaws; (b) unit volume uniformly stresse

correspond to the fracture of k small volumes elements δV) is defined in terms of the Binomial distribution[21,22]

$$\mathcal{P}(S_n = k) = \binom{n}{k} p^k (1-p)^{n-k}, \quad 0 \leq k \leq n, \tag{1}$$

where S_n denotes the total number of failures that occurred in n volumes. When k is large and p is small, by the Poison limit theorem, the distribution of the number of failures converges to a Poison distribution with parameter λ in the form

$$\mathcal{P}(S_n = k) = \frac{e^{-\lambda}\lambda^k}{k!}, \tag{2}$$

where $\lambda = kp$ is the expectation of the binomial distribution. In particular, we seek the probability that there is at least one failure. Thus, the failure probability of the unit volume has distribution

$$\mathcal{P}(S_n \geq 1) = 1 - \mathcal{P}(S_n = 0) = 1 - e^{-kp}. \tag{3}$$

To arrive at a limiting distribution for the fracture stress of a cracked solid, an appropriate functional form for the probability p is required. The following sections provide the needed forms based upon two failure models.

2.2 The weakest link (WL) model

The most widely adopted probabilistic model to describe fracture in brittle materials is based upon the weakest link (WL) theory. A central feature emerging from the WL model is the notion that catastrophic failure is driven by unstable propagation of a single microflaw contained in the unit volume V. As depicted in Fig. 2, a 'chain' analogy is then readily established. In ferritic steels, extensive work shows that cleavage microcracks propagate unstably upon attaining a critical size, $a_c = K_{Ic}^2/Y\sigma^2$, where Y represents a geometry factor, σ denotes a tensile (opening) stress acting on the microcrack plane and K_{Ic} is the material fracture toughness. A number of probabilistic approaches employ the statistics of microcracks to provide a connection between the probabilistic treatment of fracture and existing frameworks for continuum mechanics (see, for example, Beremin,[4] Wallin *et al.*,[5,6] Ruggieri and Dodds[17–19]). In the context of the present work, we avoid the micromechanics formalism of the aforementioned derivations and present a more simplified formulation for the WL model which also makes contact with the chain-of-bundle model presented next.

To arrive at a probability distribution for the fracture stress, we adopt a convenient functional form for the failure

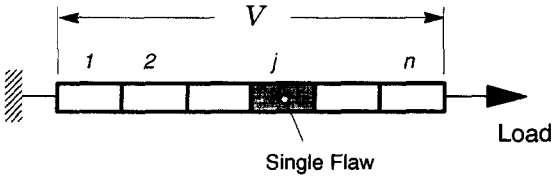

Fig. 2. Weakest link model.

probability of δV as

$$p = (\sigma_1/\sigma_s)^m, \tag{4}$$

where σ_1 is the principal stress acting on δV, m and σ_s are parameters of the function with m, $\sigma_s > 0$.

Now, substitution of eqn (4) into eqn (3) defines the failure probability $\mathcal{P}_0$ for the unit volume V in the form

$$\mathcal{P}_0 = 1 - \exp\left[-k\left(\frac{\sigma_1}{\sigma_s}\right)^m\right] = 1 - \exp\left[-\left(\frac{\sigma_1}{\sigma_u}\right)^m\right], \tag{5}$$

which is a Weibull distribution with parameters m and σ_u.

Using again weakest link arguments, we generalize the previously derived limiting distribution to any multiaxially stressed region, such as the fracture process zone ahead of a macroscopic crack or notch (see Fig. 1(a)). Here, the statistical problem of determining an asymptotic distribution for the fracture strength of the entire solid is equivalent to determining the distribution of the weakest unit volume V. The fundamental assumption is that the near-tip fracture process zone consists of N arbitrary and statistically independent unit volumes V. Consequently,

$$\mathcal{P} = 1 - [1 - \mathcal{P}_0]^N = 1 - \prod_{i=1}^{N} (1 - \mathcal{P}_0). \tag{6}$$

Substituting eqn (5) into the above expression, the probability distribution for the fracture of a cracked solid based upon the WL model is given by

$$\mathcal{P} = 1 - \exp\left[-\sum_{i=1}^{N}\left(\frac{\sigma_1}{\sigma_u}\right)^m\right], \tag{7}$$

which for $N \to \infty$ yields

$$\mathcal{P} = 1 - \exp\left[-\frac{1}{V_0}\int_\Omega \left(\frac{\sigma_1}{\sigma_u}\right)^m d\Omega\right], \tag{8}$$

where Ω denotes the volume of the near-tip fracture process zone and V_0 is a reference volume.

Following the development presented previously, the Beremin's Weibull stress[4] is then given by integration of the principal stress over the fracture process zone in the form

$$\sigma_w = \left[\frac{1}{V_0}\int_\Omega \sigma_1^m d\Omega\right]^{1/m}, \tag{9}$$

from which the limiting distribution (eqn (8)) now takes the form

$$\mathcal{P}(\sigma_w) = 1 - \exp\left[-\left(\frac{\sigma_w}{\sigma_u}\right)^m\right]. \tag{10}$$

Eqn (10) defines a two-parameter Weibull distribution[23] in terms of the Weibull modulus m and the scale factor σ_u. Previous work[4,14,15,17] has shown that m takes a value in the range 10–22 for typical structural steels.

2.3 The chain-of-bundles (CB) model

An alternative model to the WL philosophy involves relaxing the assumption that a critical microcrack triggers

catastrophic failure of the entire cracked body. When unstable propagation of a microflaw is arrested by the surrounding material (which presumably has higher fracture resistance), the distribution of local stresses accompanying the failure of a small material element containing the microflaw contributes to increase the macroscopic fracture resistance. Under increasing loading, the fracture process progresses by consecutive instability of the surviving material elements until a critical load is attained—only after a number of material elements have failed does the failure occur in a macroscopic scale, ultimately via a weakest link mechanism. In the present context, each unit volume is viewed as a chain of n statistically independent bundles, each bundle having r elements in parallel, as illustrated in Fig. 3.

We consider again a limiting distribution for the failure probability of δV. For a fiber bundle model with equal load sharing, Daniels[24] presented the first derivation of an asymptotic distribution describing the bundle strength. In his model, a single bundle has independent elements in parallel, each one with the same cross section; the load is equally redistributed among the unfailed elements when a single element fails. Let $T_1, T_2, \ldots, T_r$ denote the fracture strength of each element and let these strengths be the order statistics $T_1 \leq T_2 \leq \ldots \leq T_r$. The failure of the bundle under principal stress σ_1 satisfies the condition

$$\sigma_1 \geq \max\left\{T_1, \left(\frac{r-1}{r}\right)T_2, \ldots, \left(\frac{1}{r}\right)T_r\right\}. \tag{11}$$

When $r \to \infty$, the bundle strength is asymptotically normally distributed with expectation μ and standard deviation γ. Thus, the probability p is given by

$$p = \Phi(z) = \frac{1}{\sqrt{2\pi}} \int_{-\infty}^{z} e^{-t^2/2} dt, \tag{12}$$

where $\Phi(z)$ is the standard normal distribution function with expectation zero, standard deviation 1 and $z = (\sigma_1 - \mu)/\gamma$. Now, substitution of eqn (12) into eqn (3) defines the failure probability for the unit volume V in the form

$$\mathcal{P}_0 = 1 - \exp\left(-\frac{q}{\sqrt{2\pi}} \int_{-\infty}^{z} e^{-t^2/2} dt\right). \tag{13}$$

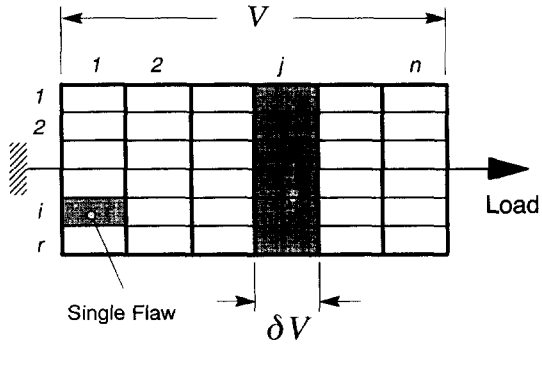

Fig. 3. Chain-of-bundles model.

Define the random variable $\mathcal{A}$ as

$$\mathcal{A} = \frac{q}{\sqrt{2\pi}} \int_{-\infty}^{z} e^{-t^2/2} dt, \tag{14}$$

which, for $q \to \infty$, has an asymptotic solution given by[25,26]

$$z = a_q + b_q \ln \mathcal{A}, \tag{15}$$

where a_q and b_q are parameters. Solving this expression for $\mathcal{A}$ and replacing z by $(\sigma_1 - \mu)/\gamma$, the limiting distribution for the fracture strength of the unit volume yields

$$\mathcal{P}_0 = 1 - \exp\left[-\exp\left(\frac{\sigma_1 - \alpha}{\beta}\right)\right], \tag{16}$$

which is a Gumbel distribution for the smallest value with location parameter α and scale parameter β.[28]

Using the parametrization

$$\sigma_1 = \ln S_1 \tag{17}$$

$$\alpha = \ln S_u$$

$$\beta = w^{-1}$$

allows eqn (16) to be written in the form

$$\mathcal{P}_0 = 1 - \exp\left[-\left(\frac{S_1}{S_u}\right)^w\right], \tag{18}$$

which is a Weibull distribution with parameters w and S_u.

Now, following the same development presented previously, the probability distribution for the fracture of cracked solid based upon the CB model becomes

$$\mathcal{P} = 1 - \exp\left[-\frac{1}{V_0}\int_{\Omega}\left(\frac{S_1}{S_u}\right)^w d\Omega\right] \tag{19}$$

where Ω denotes the volume of the near-tip fracture process zone.

Again, a stress integral having the form

$$\sigma_g = \left[\frac{1}{V_0}\int_{\Omega} S_1^w d\Omega\right]^{1/m} \tag{20}$$

is employed to recast eqn (19) as

$$\mathcal{P}(\sigma_g) = 1 - \exp\left[-\left(\frac{\sigma_g}{S_u}\right)^w\right]. \tag{21}$$

3 PARAMETER CALIBRATION AND NUMERICAL PROCEDURES

There is general agreement that the parameters of the Weibull distributions given by eqns (10) and (21) are material properties. In applications of probabilistic fracture mechanics, these parameters are generally calibrated from experimental toughness data. Beremin[4] and Minami *et al.* presented the first formalized procedures to calibrate the Weibull parameters (m, σ_u).

In related work, Ruggieri *et al.*[16] utilized their procedures to calibrate parameters (w, S_u) for a high-strength steel. More recently, Ruggieri and Dodds[17–19] implemented similar methodology in a probabilistic framework for fracture assessments of flawed structures using the research code WSTRESS.[19]

The methodology builds upon an iterative procedure incorporating a three-dimensional finite element description of the crack-tip stress fields and measured values of fracture toughness to calibrate the Weibull parameters appearing in eqns (10) and (21). Development of the numerical procedure then begins with evaluation of the stress integrals, σ_w and σ_g. These values enable construction of the evolution of σ_w (or equivalently σ_g) as deformation (loading) progresses.

For the purpose of developing a procedure to calibrate the Weibull parameters (m, σ_u) and (w, S_u), it is helpful to rewrite the probability distributions given by eqns (10) and (21) in the form

$$\mathcal{P}(\Sigma, c, b) = 1 - \exp\left[-\left(\frac{\Sigma}{b}\right)^c\right], \tag{22}$$

where $\Sigma = \sigma_w$ for the WL model and $\Sigma = \sigma_g$ for the CB model, with (c, b) denoting the corresponding Weibull parameters.

Fig. 4 summarizes the procedure to calibrate the parameters (c, b) similar to the one utilized by Ruggieri and Dodds.[19] The description that follows adopts J as the measure of macroscopic loading; the algorithm remains

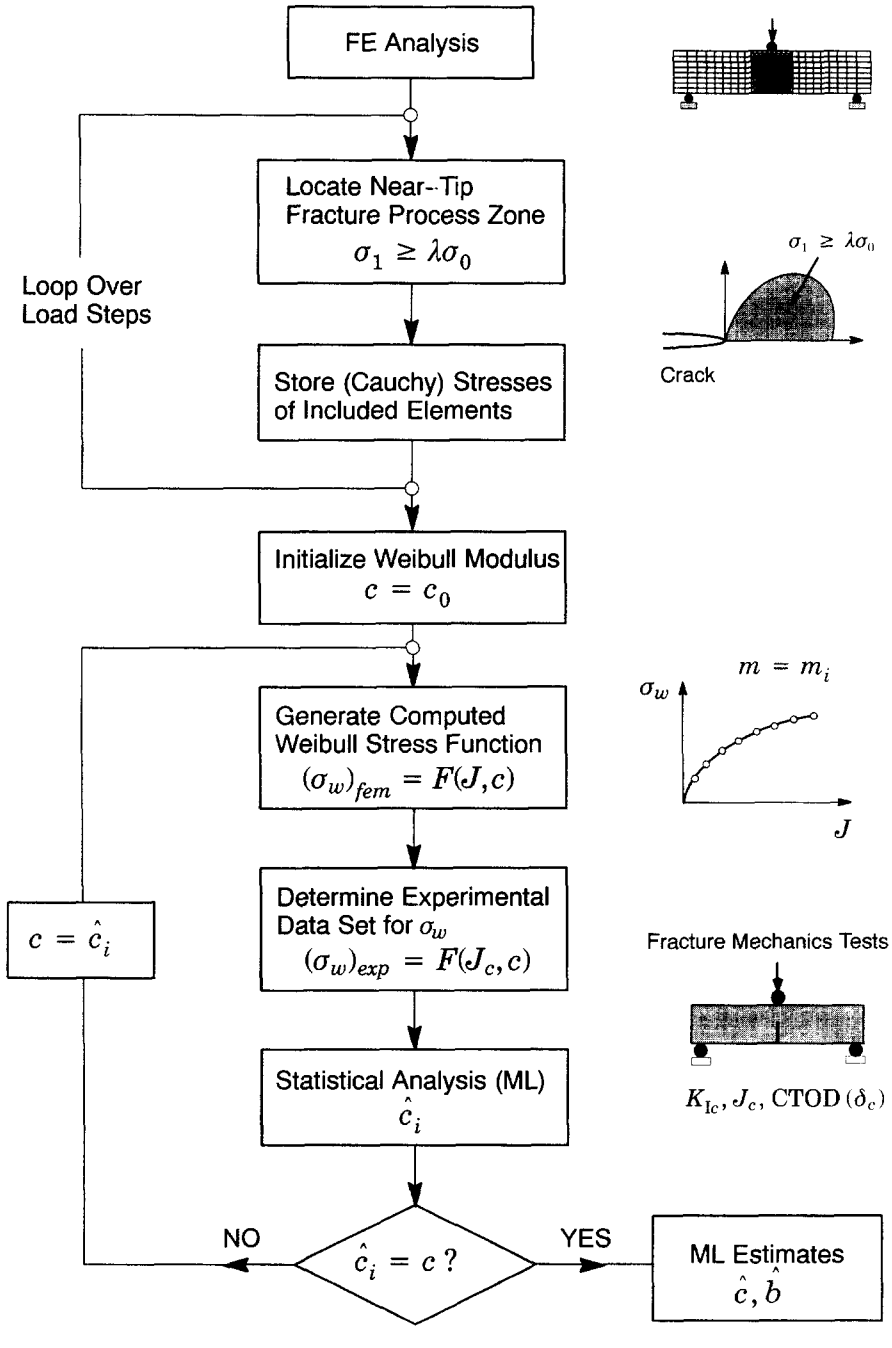

Fig. 4. Algorithm for calibration of the Weibull modulus, c.

applicable for other measures of load level, such as K or CTOD.

3.1 FE-analysis and fracture mechanics testing

Toughness data for cleavage fracture are used to define corresponding values of the Weibull stress at fracture; these values form the basis upon which the Weibull parameters for the material are estimated without making recourse to detailed micromeasurements. Crack configurations exhibiting high levels of crack tip stress triaxiality (deep notch SE(B) or C(T) fracture specimens) tested at appropriate temperatures provide cleavage fracture toughness data employed in the present procedure. Non-linear finite element analyses of the tested specimens provide the necessary stress fields and define the size of the fracture process zone for the specified load levels (here expressed by J).

The process begins by finding the material dependent value for the Weibull modulus, c, appearing in the probability distribution expressed by eqn (22). Let $\mathcal{P}_{\text{fem}}(\Sigma)$ denote the distribution of Σ corresponding to the stress state obtained through a finite element analysis. Also, let $\mathcal{P}_{\text{exp}}(\Sigma)$ denote the distribution of Σ corresponding to the measured values of fracture toughness. Since $\mathcal{P}_{\text{fem}}(\Sigma)$ and $\mathcal{P}_{\text{exp}}(\Sigma)$ have identical distributions, the calibration process becomes one of determining a set of parameters $\{c, b\}$ which satisfies this condition.

3.2 Generation of the evolution of Σ versus J

A starting value for c, denoted c_0, is required to generate the first approximation for the relationship between J in the finite element model and the stress integral, Σ, for the test specimen, expressed as $\Sigma_{\text{fem}} = F(J, m)$. This relationship is determined by numerically integrating eqns (9) and (20) at each specified load level. In isoparametric space, the current (deformed) Cartesian coordinates x_i of any point inside an eight-node tri-linear element are related to the parametric coordinates η_i using the shape functions corresponding to the kth node.[27] Let $|J|$ denote the determinant of the standard coordinate Jacobian between deformed Cartesian and parametric coordinates. Then, using standard procedures for integration over element volumes, the Weibull stress has the form

$$\sigma_w = \left[\frac{1}{V_0}\sum_{n_c}\int_{\Omega_e}\sigma_1^m \mathrm{d}\Omega_e\right]^{1/m} = \left[\frac{1}{V_0}\sum_{n_c}\int_{-1}^{1}\int_{-1}^{1}\int_{-1}^{1}\sigma_1^m |J|\mathrm{d}\eta_1\mathrm{d}\eta_2\mathrm{d}\eta_3\right]^{1/m}, \quad (23)$$

where n_c is the number of elements inside the fracture process zone near the crack tip and Ω_e is the volume of the element. The process zone used here includes all material inside the loci $\sigma_1 \geq \lambda\sigma_0$ with $\lambda \approx 2$. For computational simplicity, an element is included in the fracture process zone if the σ_1 computed at $\eta_1 = \eta_2 = \eta_3 = 0$ exceeds $\lambda\sigma_0$.

Similarly, the finite element form in parametric space for the stress integral σ_g is given by

$$\sigma_g = \left[\frac{1}{V_0}\sum_{n_c}\int_{\Omega_e}S_1^w \mathrm{d}\Omega_e\right]^{1/w} = \left[\frac{1}{V_0}\sum_{n_c}\int_{-1}^{1}\int_{-1}^{1}\int_{-1}^{1}S_1^w |J|\mathrm{d}\eta_1\mathrm{d}\eta_2\mathrm{d}\eta_3\right]^{1/w}, \quad (24)$$

where again the process zone includes all material inside the loci $\sigma_1 \geq \lambda\sigma_0$, with $\lambda \approx 2$.

3.3 Evaluation of Σ at fracture

The computed relationship between J and Σ then enables evaluation of the stress integral at fracture, denoted Σ_{exp} corresponding to each experimental fracture toughness value, J_c. This is accomplished by evaluating $\Sigma_{\text{exp}} = F(J_c, m)$ using the functional form between J and Σ_{fem}. In practice Σ_{exp} are evaluated from a simple interpolation employing discrete values of Σ_{fem} versus J. The Σ_{exp} values then define a statistical sample with distribution $\mathcal{P}_{\text{exp}}(\Sigma)$. A statistical analysis based upon the maximum likelihood method for this distribution yields the 'new' estimate of the Weibull modulus, $\hat{c}_1$. Convergence is attained if $|\hat{c}_{i-1} - \hat{c}_i| \leq \epsilon$ otherwise the process starts anew with the distribution $\mathcal{P}_{\text{fem}}(\Sigma)$ computed for $c = \hat{c}_i$.

3.4 Numerical modeling of ductile tearing

A key feature of the present methodology is the inclusion of ductile tearing effects in the probabilistic formulation using numerical modeling of stable crack growth that often precedes cleavage fracture in ferritic steels. The computational cell methodology proposed by Xia and Shih[35–37] provides a model for ductile crack extension that includes a realistic void growth mechanism, and a microstructural length-scale physically coupled to the size of the fracture process zone. Void growth remains confined to a layer of material symmetrically located about the crack plane, as illustrated in Fig. 5(a), and having thickness D, where D is associated with the mean spacing of the larger, void initiating inclusions. This layer consists of cubical cell elements with dimension D on each side; each cell contains a cavity of initial volume fraction f_0 (the initial void volume divided by cell volume). As a further simplification, the void nucleates from an inclusion of relative size f_0 immediately upon loading. Progressive void growth and subsequent macroscopic material softening in each cell are described with the Gurson–Tvergaard (GT) constitutive model for dilatant plasticity.[38,39] When f in the cell incident on the current crack tip reaches a critical value, f_E, the computational procedures remove the cell thereby advancing the crack tip in discrete increments of the cell size. Material outside the computational cells, the 'background' material, follows a conventional J_2 flow theory of plasticity and remains undamaged by void growth in the cells.

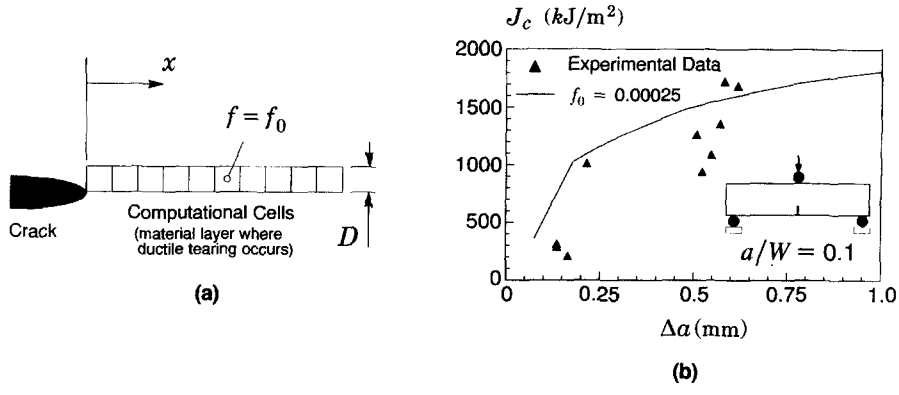

Fig. 5. (a) Model for ductile crack growth using computational cells. (b) Computed crack growth resistance curve for the SE(B) specimen with $a/W = 0.1$.

Material properties required for this methodology include: for the background material Young's modulus (E), Poison's ratio (ν), yield stress (σ_0) and hardening exponent (n) or the actual measured stress–strain curve; and for the computational cells: D and f_0 (and of much less significance f_E). The background material and the matrix material of the cells generally have identical flow properties. Using an experimental $J - \Delta a$ curve obtained from a conventional SE(B) or C(T) specimen, a series of finite element analyses of the specimen are conducted to calibrate values for the cell parameters D and f_0 which bring the predicted $J - \Delta a$ curve into agreement with experiment. The CTOD at initiation of ductile tearing provides a good starting value for D, with f_0 then varied to obtain agreement with the experiment. Alternatively, metallurgical surveys of inclusion volume fractions and sizes may be used with various packing arrangements (e.g. nearest neighbor distance) to estimate D and/or f_0. Experience with plane-strain finite element analyses of SE(B) and C(T) specimens to estimate D and f_0 for common structural and pressure vessel steels suggests values of 50–200 μm for D, 0.001–0.005 for f_0, with f_E typically 0.15–0.20. Once determined in this manner using a specific experimental R-curve, D and f_0 become 'material' parameters and remain fixed in analyses of all other specimen geometries for the same material.

4 PREDICTION OF FRACTURE PROBABILITY

The probabilistic methodology outlined in the previous sections has been applied to predict effects of specimen geometry on measured values of toughness values. Such an application serves as a prototype for a wide class of engineering problems involving the transferability of fracture toughness data from laboratory specimens to structural components. Fracture mechanics tests on conventional SE(B) specimens (plane-sided) with varying crack length to width ratios, a/W, provide the experimental cleavage fracture toughness data employed in this study. Testing of these specimens was carried out at -120°C for a deep crack ($a/W = 0.5$) and for a shallow crack ($a/W = 0.1$) configuration.[30] The specimens have a loading span, $S = 120$ mm, a width, $W = 30$ mm, and thickness $B = 15$ mm (see Fig. 6). The material is a high-strength, low-alloy

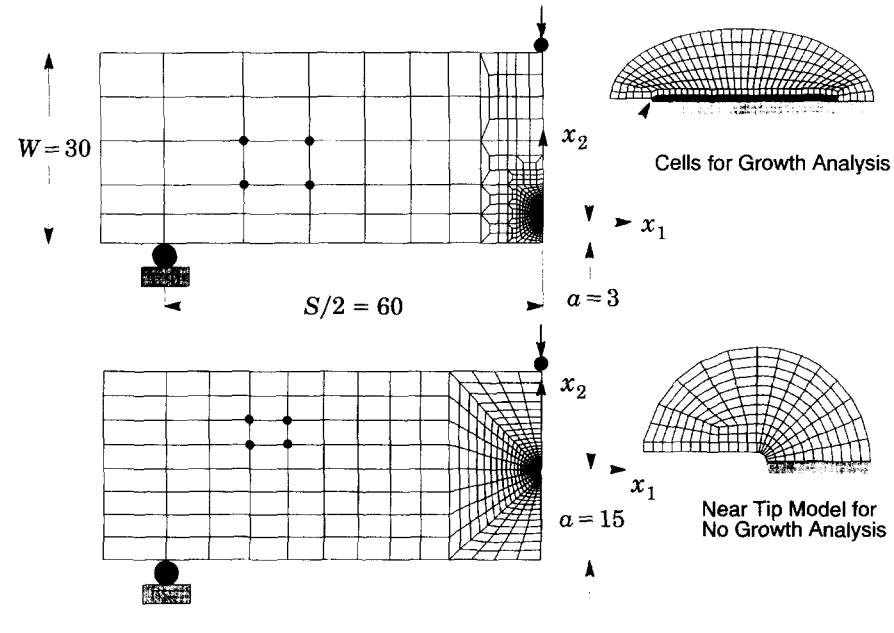

Fig. 6. Finite element models for three-point SE(B) specimens: (a) $a/W = 0.1$; (b) $a/W = 0.5$ (all units in millimeters).

(HSLA) steel (663 MPa yield stress) with relatively low strain hardening (tensile strength/yield strength = 1.08). Fig. 7(a) reveals the pronounced effect of a/W ratio and ductile growth on experimental fracture toughness values (J_c). Most of the specimens with $a/W = 0.1$ experienced ductile crack extensions (Δa) of 0.5–0.75 mm prior to cleavage fracture. In contrast, specimens with $a/W = 0.5$ exhibited completely brittle behavior with no measurable crack extension prior to cleavage fracture. Fig. 7(b) displays the Weibull distribution of the toughness data for the SE(B) specimens. The Weibull shape parameter for both distributions is in agreement with the value of 2 given by Wallin;[6] this value describes the ('theoretical') scatter of J_c for cleavage fracture in ferritic steels.

Finite element analyses conducted on plane-strain models for the deep and shallow notch specimens provide the crack front stresses for evaluation of the stress integrals given by eqns (23) and (24). Ruggieri and Dodds[17] present details of the analyses and computational procedures. Fig. 6 shows the finite element models, dimensions and boundary conditions. The models have one-layer of elements in the thickness direction with plane strain conditions ($x_3 = 0$) imposed on all nodes and sufficient mesh refinement near the tip to provide adequate solution of the stress fields. Numerical computations were performed in a finite strain setting by the WARP3D finite element code.[31] J-integral values are obtained using the domain integral facility available in WARP3D. As noted previously, stable crack growth prior to cleavage fracture occurs in the shallow notched specimens. Consequently, prediction of toughness results for these specimens requires inclusion of crack growth modeling in the probabilistic formulation. Here, the analyses consider a stationary crack (with crack tip mesh similar to the one employed for the deep notch specimen) and a growing crack analysis which accommodates ductile tearing with the computational cell scheme previously outlined. The constitutive model adopted in the analyses follows a J_2 flow theory with Mises yield criterion. The uniaxial true stress–logarithmic strain response for the material is modeled with a piecewise linear approximation to the mechanical tensile behavior.[17]

The computational cell approach requires calibration of the initial porosity, f_0, and cell size, D, from a measured set of R-curves. As noted by Ruggieri and Dodds,[20] calibration of the cell parameter, f_0, using the load versus load-line displacement exhibit essentially no sensitivity on this parameter—crack growth resistance curves exhibit a much stronger sensitivity to f_0 as required to define a robust calibration procedure. Ideally, R-curves obtained using $a/W = 0.5$ specimens would be used for this procedure. However, deep-crack specimen R-curves are not available from the experimental investigation—at the test temperature, no ductile tearing occurs. Alternatively, experimental R-curves for other, low constraint geometries would be suitable to perform the calibration. Here, only the shallow-crack data is available and we use it to perform calibration of the computational cell parameters (D, f_0). Fig. 5(b) shows the measured cleavage fracture data for the shallow-crack specimens plotted in an R-curve format. The computed resistance curve shown on this figure is obtained using the values $D = 200$ μm and $f_0 = 0.00025$ in the finite element analysis for ductile crack growth. Despite the relative scatter observed in the experimental (cleavage) values, the predicted R-curve captures the average evolution of crack growth behavior.

The research code WSTRESS[19] is used to determine the material dependent value for the shape parameter m and w appearing in eqns (23) and (24). After convergence is attained, a small sample correction is applied to the maximum likelihood estimate of m using appropriate unbiasing factors given by Thoman *et al.*[29] Using the calibration procedure outlined in previous section and employing the measured fracture toughness for the deep-notched SE(B) specimens ($a/W = 0.5$), m has the value of 15.6 with 90% confidence intervals given by (9.0, 20.9) and w has the value of 7.9 with 90% confidence intervals given by (4.5, 10.5).

With the Weibull modulus m and w calibrated, we predict the combined effects of a/W ratio and ductile tearing for the experimental cleavage fracture toughness data using a toughness scaling procedure presented by Ruggieri and Dodds.[17,19] Fig. 8(a) and (b) show the computed evolution of σ_w and σ_g, under increasing values of J, for the deep and shallow crack configurations. The stress integrals are

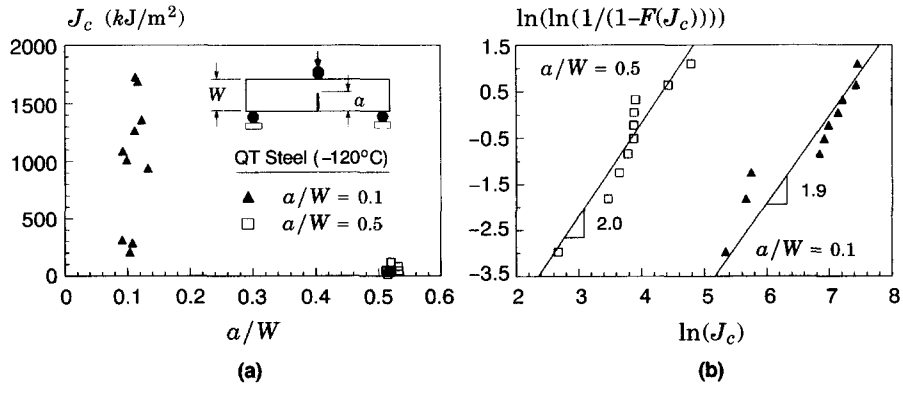

Fig. 7. (a) Experimental cleavage fracture toughness data (SE(B) test results) for QT steel at − 120°C. (b) Two-parameter Weibul distribution of toughness data for SE(B) specimens.

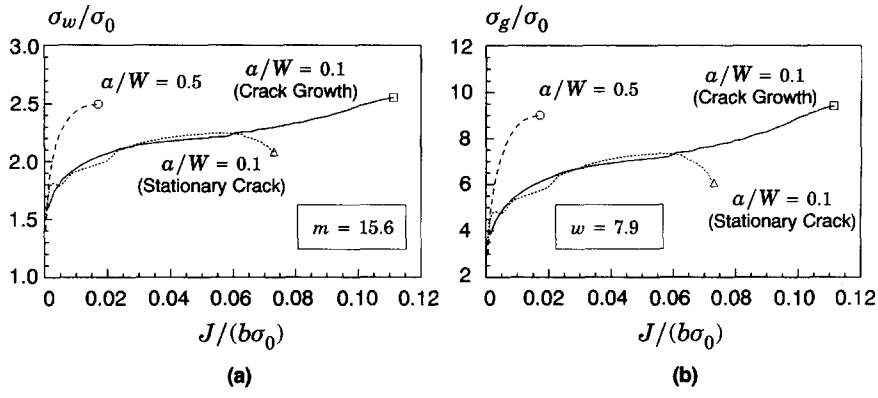

Fig. 8. Variation of the stress Σ with increasing load for the SE(B) specimens: (a) weakest link model (σ_w); (b) chain-of-bundles model (σ_g).

normalized by the yield stress, σ_0, for the material under consideration while the loading parameter, J, is normalized by the remaining crack ligament of the specimen, $b = W - a$, and σ_0. Although not explicitly addressed here, we note that σ_g may display more sensitivity to mesh details and mesh resolution (particularly near the crack tip) than σ_w as the integral given by eqn (24) involves a power of $\exp(\sigma_1)$—a finer mesh may be required to resolve more accurately the near-tip stress fields. Since our primary interest lies in comparing the response of both failure models in predicting the toughness distribution for the shallow crack specimen, the mesh employed in the analyses appears satisfactory.

The stress integrals and σ_g increase monotonically for the SE(B) specimens with $a/W = 0.5$ which reflect the increase in the near-tip stress fields as loading progresses. By contrast, σ_w and σ_g for the stationary crack analysis of the SE(B) specimen with $a/W = 0.1$ also increase monotonically at early stages of loading, but sharply decrease after a 'saturation' level is reached at $J/(b\sigma_0) \approx 0.05$. This behavior is caused by severe loss of crack-tip constraint, with consequent reduction in the stress levels ahead of the crack tip, experienced by such crack configuration as loading progresses (see Dodds *et al.*[32] and Ruggieri and Dodds[17]). However, inclusion of ductile crack growth in the analysis counteracts the effects of constraint loss and, thus, restores σ_w and σ_g to high constraint levels, as observed in Fig. 8. These trends are fully consistent with those obtained in previous numerical analyses[33,34] in that stable crack growth elevates the near-tip stresses and increases the volume of the cleavage fracture process zone, thereby increasing the stress integrals σ_w and σ_g.

The curves presented in Fig. 8 provide the distribution of a continuous function of Σ-values at fracture for these specimens. The generated, continuous function of Σ-values (σ_w or σ_g) at fracture for the SE(B) specimens with $a/W = 0.5$ (configuration A) is 'transferred' for constraint loss and crack extension to predict the distribution of J_c-values for the shallow-crack specimens with $a/W = 0.1$ (configuration B). The probability distribution of cleavage fracture toughness for configuration B is then expressed in closed form as

$$P(J_c^B) = 1 - \exp\left[-\left(\frac{F_B(J_c^B, c)}{b}\right)^c\right], \tag{25}$$

where $F_B(J, c)$ denotes the computed functional relationship between J (or equivalently CTOD) in configuration B (finite element model) and the stress integral Σ for the calibrated value of c.

The Weibull probability plot in Fig. 9(a) and (b) shows the predicted distributions and 90% confidence bounds of cleavage fracture toughness for the SE(B) specimen with $a/W = 0.1$ using both failure models. The solid symbols in the plots indicate the experimental fracture toughness data for those specimens. Values of cumulative probability, F, are obtained by ordering the J_c-values and using $F = (i - 0.5)/$

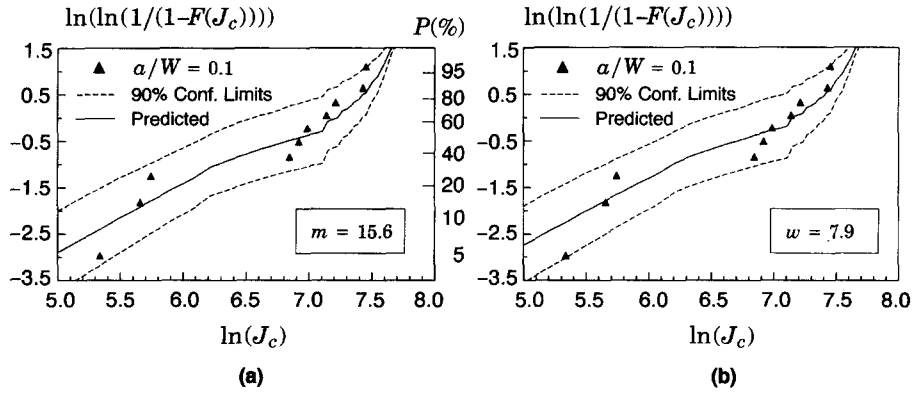

Fig. 9. Prediction of the probability distribution for the cleavage fracture toughness data of SE(B) specimens with $a/W = 0.1$. (a) Weakest link model (σ_w). (b) Chain-of-bundles model (σ_g).

N, where i denotes the rank number and N defines the total number of experimental toughness values. The predicted curves are generated from the point estimate and 90% confidence limits for the parameters (c, b) of the SE(B) specimen with $a/W = 0.5$.

The good agreement between the predicted distributions displayed in Fig. 9 and the experimental data (note that all measured J_c-values lie within the 90% confidence bounds) indicates the robustness of the present probabilistic methodology. An interesting feature of the results displayed in Fig. 9 is that the predicted distributions for the WL and CB model are very similar. Such a behavior suggests that use of the more refined chain-of-bundles model does not provide any real improvement in the transferability procedure. However, inclusion of ductile crack growth in the computation of the stress $\Sigma(\sigma_w$ and $\sigma_g)$ proves essential to predict the fracture toughness values in the upper tail of the curves (i.e. J_c-values > 1000–1200 kJ/m^2). This is clearly evidenced by examining the evolution of σ_w and σ_g with loading (J) in Fig. 8. The stationary crack (no-growth) analysis provides, at best, predicted J_c-values for the lower tail of the curves (< 1000).

5 CONCLUDING REMARKS

This study describes a probabilistic framework for brittle fracture using two failure models: weakest link and chain-of-bundles approaches. The weakest link philosophy is defined such as fracture of a small element at the microlevel of material ahead of a macroscopic crack triggers general catastrophic failure. The chain-of-bundles approach allows one or more failures at the microlevel of near-tip material before catastrophic fracture occurs. The probability distributions for both models are cast into a two-parameter Weibull distribution of the fracture stress. A numerical procedure to calibrate the Weibull parameters based upon measured toughness values and finite element solutions is then presented. Application of the proposed methodology to analyze the fracture behavior of a high-strength, low-alloy steel successfully transfer measured toughness values across different structural geometries and crack configurations. Moreover, the probabilistic fracture parameters σ_w and σ_g incorporate both the effects of stressed volume and the potentially strong changes in the character of the near-tip stress fields owing to constraint loss and ductile crack extension. Current work is in progress to extend the present framework as a broader predictive methodology to assess structural integrity.

ACKNOWLEDGEMENTS

This investigation was supported by grants principally from Fundação de Amparo à Pesquisa do Estado de São Paulo—FAPESP (grant 95-9898-0). Computational support for software development was provided by the High Performance Computation Center (LCCA) of the University of São Paulo.

REFERENCES

1. Batdorf, S. B. and Crose, J. G. A statistical theory fo the fracture of brittle structures subjected t nonuniform polyaxial stresses. *Journal of Applie Mechanics*, 1974, **41**, 459–464.
2. Evans, A. G. A general approach for the statistica analysis of multiaxial fracture. *Journal of Americar Ceramic Society*, 1978, **61**, 302–308.
3. Matsuo, Y. Statistical theory for multiaxial stress state using Weibull's three-parameter function. *Engineerin Fracture Mechanics*, 1981, **14**, 527–538.
4. Beremin, F. M. A local criterion for cleavage fractur of a nuclear pressure vessel steel. *Metallurgica Transactions*, 1983, **14A**, 2277–2287.
5. Wallin, K., Saario, T. and Törrönen, K. Statistica model for carbide induced brittle fracture in steel *Metal Science*, 1984, **18**, 13–16.
6. Wallin, K. The scatter in K_{Ic} results. *Engineerin Fracture Mechanics*, 1984, **19**, 1085–1093.
7. Wallin, K., Saario, T., Törrönen, K. and Forstén, J. Brittle fracture theory (WST model). In *Reliabilit of Reactor Materials. Fracture Mechanics* Research Report 402, eds. K. Törrönen and I Aho-Mantila, Technical Research Center o Finland, 1986.
8. Wallin, K., Statistical aspects of constraint wit emphasis on testing and analysis of laborator specimens in the transition region. In *Constrain Effects in Fracture, A.STM STP 11 71*, eds. Hacket et al., American Society for Testing and Materials Philadelphia, PA, 1993, pp. 264–288.
9. Lin, T., Evans, A. G. and Ritchie, R. O. A statistica model of brittle fracture by transgranular cleavage *Journal of Mechanics and Physics of Solids*, 1986 **21**, 263–277.
10. Brúckner-Foit, A., Ehl, W., Munz, D. and Trolldenier B. The size effect of microstructural implications o the weakest link model. *Fatigue and Fracture o Engineering Materials and Structures*, 1990, **13** 185–200.
11. Godse, R. and Gurland, J., A statistical model for lov temperature cleavage fracture in mild steels, *Act Metallurgica*, **37**, 541–548.
12. Mudry, F. A local approach to cleavage fracture *Nuclear Engineering and Design*, 1987, **105**, 65–76.
13. Bakker, A. and Koers, R. W. J., Prediction o cleavage fracture events in the brittle-ductil transition region of a ferritic steel. In *Defec Assessment in Components—Fundamentals an Applications*, ESIS/EG9, eds. Blauel and Schwalbe Mechanical Engineering Publications, London, 1991 pp. 613–632.
14. Minami, F., Brückner-Foit, A., Munz, D. an Trolldenier, B. Estimation procedure for the Weibul parameters used in the local approach. *Internationa Journal of Fracture*, 1992, **54**, 197–210.
15. Ruggieri, C., Minami, F. and Toyoda, M., The loca

approach to the effect of notch depth on fracture toughness. In *9th European Conference on Fracture (ECF9)*, Vol. 1.I, Varna, Bulgaria, 1992, pp. 621–626.
16. Ruggieri, C., Minami, F. and Toyoda, M. A statistical approach for fracture of brittle materials based on the chain-of-bundles model. *Journal of Applied Mechanics*, 1995, **62**, 320–328.
17. Ruggieri, C. and Dodds, R. H. A transferability model for brittle fracture including constraint and ductile tearing effects: a probabilistic approach. *International Journal of Fracture*, 1996, **79**, 304–340.
18. Ruggieri, C. and Dodds, R. H., Probabilistic modeling of brittle fracture including 3-D effects on constraint loss and ductile tearing. In *International Conference on Local Approach to Fracture (MECAMAT 96)*, Fontainebleau, France, 1996.
19. Ruggieri, C. and Dodds, R. H., WSTRESS Release 1.0: numerical computation of probabilistic fracture parameters for 3-D cracked solids, Technical Report BT-PIVV-30, University of São Paulo.
20. Ruggieri, C., Panontin, T. L. and Dodds, R. H. Numerical modeling of ductile crack growth in 3-D using computational cells elements. *International Journal of Fracture*, 1996, **82**, 67–95.
21. Feller, W., *Introduction to Probability Theory and Its Application*, Vol. I, Wiley, New York, 1957.
22. Kendall, M. G. and Stuart, A., *The Advanced Theory of Statistics*, 2nd edn, Hafner, New York, 1967.
23. Weibull, W. The phenomenon of rupture in solids. *Ingeniors Vetenskaps Akademien, Handlingar*, 1939, **153**, 55.
24. Daniels, H.E. The statistical theory of the strength of bundles of threads. *Proceedings of the Royal Society of London, Series A*, 1945, **183**, 405–435.
25. Epstein, B. Elements of the theory of extreme values. *Technometrics*, 1960, **2**, 27–41.
26. Cramér, H., *Mathematical Methods of Statistics*, Princeton University Press, NJ, 1946.
27. Zienkiewicz, O. C., *The Finite Element Method*, 3rd edn, McGraw-Hill, London, 1989.
28. Mann, N. R., Schafer, R. E. and Singpurwalla, N. D., *Methods for Statistical Analysis of Reliability and Life Data*, Wiley, New York, 1974.
29. Thoman, D. R., Bain, L. J. and Antle, C. E. Inferences on the parameters of the Weibull distribution. *Technometrics*, 1969, **11**, 445–460.
30. Toyoda, M., Minami, F. and Matsuo, T. Hagiwara, Y and Inoue, T., Effect of work hardening properties of high strength steels on cleavage/ductile fracture resistance. *Prep. National Meeting of the Japan Welding Society*, 1991, **49**, 112–113. in Japanese.
31. Koppenhoefer, K., Gullerud, A., Ruggieri, C., Dodds, R. and Healy, B., WARP3D: Dynamic Nonlinear Analysis of Solids Using a Preconditioned Conjugate Gradient Software Architecture, Structural Research Series (SRS) 596, UILU-ENG-94-2017, University of Illinois at Urbana-Champaign, 1994.
32. Dodds, R. H., Anderson, T. L. and Kirk, M. T. A framework to correlate *a/W* ratio effects on elastic-plastic fracture toughness (J_c). *International Journal of Fracture*, 1991, **48**, 1–22.
33. Varias, A. G. and Shih, C. F. Quase-static crack advance under a range of constraints—steady state fields based on a characteristic length. *Mechanics and Physics of Solids*, 1993, **41**, 835–861.
34. Dodds, R. H., Tang, M. and Anderson, T. L., *Effects of Prior Tearing on Cleavage Fracture Toughness in the Transition Region in Constraint Effects in Fracture, Theory and Application*, ASTM STP 1244, eds. M. Kirk and A. Bakker, American Society for Testing and Materials, Philadelphia, PA, 1993.
35. Xia, L. and Shih, C. F. Ductile crack growth—I. A numerical study using computational cells with microstructurally-based length scales. *Journal of the Mechanics and Physics of Solids*, 1995, **43**, 233–259.
36. Xia, L. and Shih, C. F. Ductile crack growth—II. Void nucleation and geometry effects on macroscopic fracture behavior. *Journal of the Mechanics and Physics of Solids*, 1995, **43**, 1953–1981.
37. Xia, L. and Shih, C. F. Ductile crack growth—III. Statistical aspects of cleavage fracture after tearing. *Journal of the Mechanics and Physics of Solids*, 1996, **44**, 603–639.
38. Gurson, A. L., Continuum theory of ductile rupture by void nucleation and growth: part I—yield criteria and flow rules for porous ductile media, *Journal of Engineering Materials and Technology*, **99**, 2–15.
39. Tvergaard, V. Material failure by void growth to coalescence. *Advances in Applied Mechanics*, 1990, **27**, 83–151